Vision-Based Robot Motion Control System by Using a SOPC System

Yi-Shiun Lin, Yi-Ting Chen, and Ching-Long Shih

Department of Electrical Engineering, National Taiwan University of Science and Technology

Abstract— **This thesis presents a SOPC-based servo motion control technique for the robot manipulator system. The system adopts MATLAB to perform image processing functions, such as the transformation of the color space, morphological operation, data classification of the object, the shape recognition and endpoint detection. For the servo motion control of the robotic system, it consists of two controller modules. The first one control module is consisted of quadrature encoder pulse circuits, limit switches detection, generation of pulse width modulation ,and point-to- point motion trajectory generator. Then, control signals are sent via FPGA to drive circuits for controlling each motor. The other module which includes a user interface and calculation of inverse kinematics, which is implemented via the NIOS II.**

Finally, user can send commands via PC to perforem the shape recognition, data classification of the object's color, and play tic-tac-toe games on the basis of image processing. The experimental results have demonstrated the effectiveness and validity of the proposed FPGA system applied on the servo motion control of the robot manipulator system.

Keywords— **SOPC; Arm Robot Motion Control; Image Processing**

I. INTRODUCTION

Manipulator servo control system architecture shown in Figure 1. In ALTERA DE2-70 development board for the control of the core, control signals from the DE2-70 development board to the DC motor drives by DE2-70 development board detection of each axis motor position feedback signal, the completion of position servo control. With MATLAB realize image processing and human interface design, so manipulator object color and shape recognition Tic Tac Toe game.

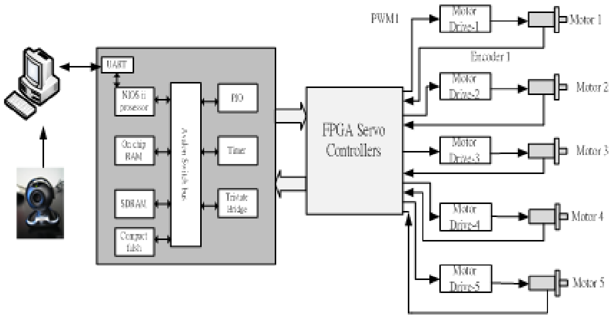

Figure 1. System Architecture

II. SOC DESIGN AND PLANNING

A. Introduction

Manipulator control system required hardware and software design of control principle and hardware aspects include a digital low-pass filter, optical encoder decoder circuit, pulse width modulation circuit, trajectory generator, digital PID controller, the software aspects human-computer interface design, reverse kinematics, point to point trajectory generator, NIOS II microprocessor with hardware specifications to be able to properly access the circuit registers.

B. S-Curve

Plane or space curve often describes polynomial notation , however , can only be used to describe a polynomial linear , second order polynomial can only describe parabolic curve , so the plane or space to describe any curve at least need to use third-order (more) polynomial . Applied to the actual motion control system for planning the path curve , since the characteristics of the motor mechanism , most probably organic table speed , acceleration, jerk limits , so the machine to be smooth in operation , reduced vibration , only the position must be continuous , must also consider the rate of continuous , continuous acceleration , jerk even be considered , or excessive acceleration or velocity may cause damage to the machine . Therefore, the success of the control acceleration and deceleration and speed commands are closely related , based on the above considerations, the first-order and second-order polynomial are not enough to describe the plane or space curve ; while the cubic polynomial to reach the position, velocity , and acceleration of continuous features. Of course, the higher order polynomial can achieve the same or even better results, but higher order polynomial time required to calculate the longer chips will consume too much resources. In this article on the S -curve velocity profiles as a curve trajectory planning .

DDA command pulse is the pulse wave cycle times even sent , the input frequency is fixed , if a variable frequency, the counter may be incremented with the input frequency change speed , it is desirable produce a S-curve characteristic of the counter , with the digital difference analysis method can be achieved with acceleration, constant velocity , deceleration pulse command , Figure 2 is a simulation result.

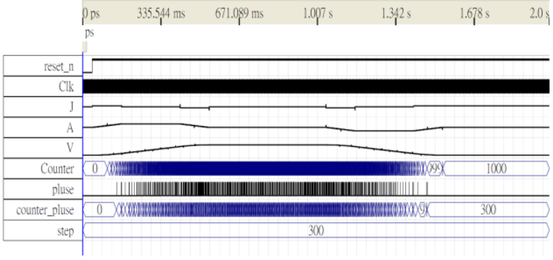

Figure 2. S-curve velocity profiles simulated results

C. Forward Kinematics

DH parameters using the forward kinematics this method, the joint angle (joint angle) of the z-axis represents the rotation angle of the connecting rod offset (link offset) extending in the z-axis represents the distance of the length of the link (link length) length in the direction of x-axis, the twist angle of the link (link twist) represents the x-axis rotation angle. Table 1 shows the five-axis manipulator DH parameter table, Figure 3 shows the DH parameters defined coordinates.

TABLE 1: DH PARAMETER TABLE

	θ_i	d_i	a_i	α_i
1	θ_1	d_1	0	-90
2	θ_2	0	a_2	0
3	θ_3	0	a_3	0
4	θ_4	0	a_4	-90
5	θ_5	d_5	0	0

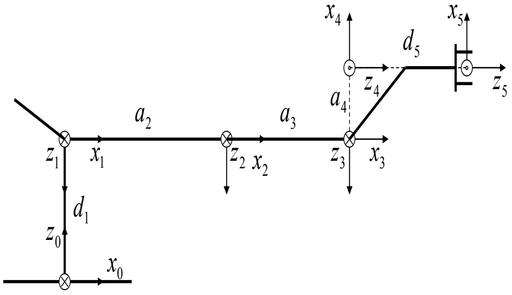

Figure 3. DH parameters defined coordinates

$$ {}^{0}T_1 = \begin{bmatrix} C_1 & 0 & -S_1 & 0 \\ S_1 & 0 & C_1 & 0 \\ 0 & -1 & 0 & d_1 \\ 0 & 0 & 0 & 1 \end{bmatrix} \quad {}^{1}T_2 = \begin{bmatrix} C_2 & -S_2 & 0 & a_2C_2 \\ S_2 & C_2 & 0 & a_2S_2 \\ 0 & 0 & 1 & 0 \\ 0 & 0 & 0 & 1 \end{bmatrix} $$

$$ {}^{2}T_3 = \begin{bmatrix} C_3 & -S_3 & 0 & a_3C_3 \\ S_3 & C_3 & 0 & a_3S_3 \\ 0 & 0 & 1 & 0 \\ 0 & 0 & 0 & 1 \end{bmatrix} \quad {}^{3}T_4 = \begin{bmatrix} C_4 & 0 & -S_4 & a_4C_4 \\ S_4 & 0 & C_4 & a_4S_4 \\ 0 & -1 & 0 & 0 \\ 0 & 0 & 0 & 1 \end{bmatrix} \quad (1) $$

$$ {}^{4}T_5 = \begin{bmatrix} C_5 & -S_5 & 0 & 0 \\ S_5 & C_5 & 0 & 0 \\ 0 & 0 & 1 & d_5 \\ 0 & 0 & 0 & 1 \end{bmatrix} $$

$$ {}^{0}T_5 = {}^{0}T_1 {}^{1}T_2 {}^{2}T_3 {}^{3}T_4 {}^{4}T_5 = \begin{bmatrix} R_{3\times3} & & & R_{4\times1} \\ 0 & 0 & 0 & 1 \end{bmatrix} $$

After the commencement of five-axis manipulator DH parameters can be expressed as:

D. Inverse Kinematics

Mechanical arm position servo control, mainly the use of counter-movement to release the joint angles calculated position command, but because the results are not the only solution, they need to verify its forward kinematics calculations. In the reverse kinematics must be set before the end of the arm posture and terminal α-axis angle of rotation β, the inverse kinematics to the formula (2) can be rewritten and expressed by the formula (3):

$$P_{4\times1}=\begin{bmatrix} C_1(a_2C_2+a_3C_{23}+a_4C_{234}-d_5S_{23}4) \\ S_1(a_2C_2+a_3C_{23}+a_4C_{234}-d_5S_{234}) \\ d_1-a_2S_2-a_3S_{23}-a_4S_{234}-d_5C_{234} \\ 1 \end{bmatrix} \quad (2)$$

$$\begin{aligned} &C_1(L_2C_2+L_3C_{23}+L_4C_{234}-L_5S_{23}4)=x \\ &S_1(L_2C_2+L_3C_{23}+L_4C_{234}-L_5S_{234})=y \\ &L_1-L_2S_2-L_3S_{23}-L_4S_{234}-L_5C_{234}=z \qquad (3) \\ &\theta_2+\theta_3+\theta_4=\alpha \\ &\theta_5=\beta \end{aligned}$$

The formula (3) can be obtained after the operation after the value of the joint angle:

$$\begin{aligned} &\theta_1=\tan^{-1}(\frac{y}{x}) or \tan^{-1}(\frac{y}{x})+\pi \\ &\theta_2=\tan^{-1}(\frac{\sin\theta_2}{\cos\theta_2}) \\ &\theta_3=\pm\cos^{-1}(\frac{x^{-2}+z^{-2}-a_2{}^2-a_3{}^2}{2a_2a_3}) \\ &\theta_4=\alpha-\theta_2-\theta_3 \\ &\theta_5=\beta \end{aligned}$$

Due to the general use of anti- kinematic conditions must be given first gesture , but the actual use will find the use of forward kinematics can be obtained directly , but no solution but it will reverse kinematics situation. The possible reasons for the movable arm beyond the scope or α worth incorrectly set no solution. Anti-kinematics process of discovery, will produce no solution because α settings cause cos ^ (-1) calculation error , cos ^ (-1) can only calculation is less than -1 or greater than 1 , as long as the excess this range will be no solution , so for this problem , this paper uses given in advance posture α value, and then use iteration to choose a more appropriate value.

In application, the first arm activities to identify the relationship between the α value , described in Figure 3 in the end position when the arm falls within the boundaries of the left or right , α value will be adjusted appropriately . In addition, after the forward kinematics coordinate value after verification , if more than 1mm away with the command position must be re- iterative solution correction value α , Figure 4 is a microprocessor in the practical implementation of NIOS result, the input command x = 350, y = 0, z = 200, alpha = 0 ° , but this command has exceeded the robot activities , not perpendicular to the desktop attitude , through iterative calculation results after the x = 350, y = 0, z = 200, alpha = 15 ° , Figure 5 shows the results back to the NIOS microprocessor control panel.

Figure 3 and the α value of the relationship arm

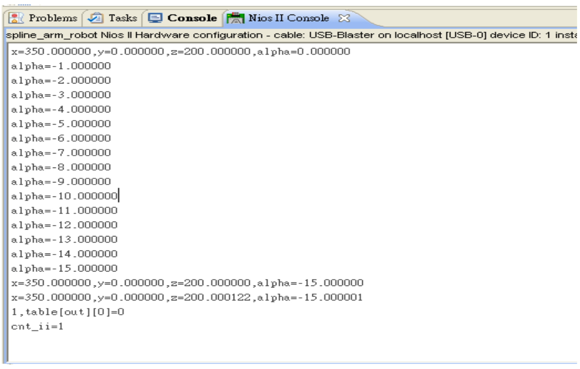

spline_arm_robot Nios II Hardware configuration - cable: USB-Blaster on localhost [USB-0] device ID: 1 insta

```
x=350.000000,y=0.000000,z=200.000000,alpha=0.000000
alpha=-1.000000
alpha=-2.000000
alpha=-3.000000
alpha=-4.000000
alpha=-5.000000
alpha=-6.000000
alpha=-7.000000
alpha=-8.000000
alpha=-9.000000
alpha=-10.000000
alpha=-11.000000
alpha=-12.000000
alpha=-13.000000
alpha=-14.000000
alpha=-15.000000
x=350.000000,y=0.000000,z=200.000000,alpha=-15.000000
x=350.000000,y=0.000000,z=200.000122,alpha=-15.000001
1,table[out][0]=0
cnt_ii=1
```

Figure 4. the results of anti-kinematics

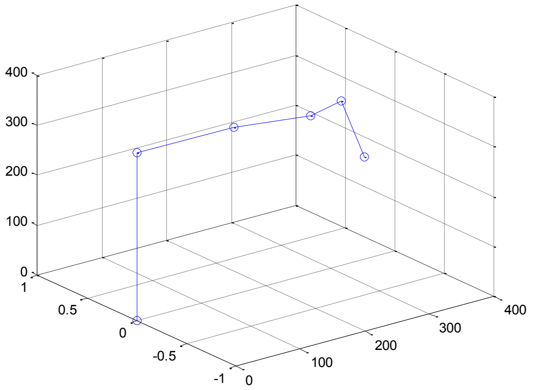

Figure 5. Schematic arm gesture

III. Computer Vision and Image Processing

A. Object color recognition

Mostly on color recognition processing using a fixed threshold, the desired color of the object is filtered out; but under different light sources, shadows caused by reflection and often result in false positives. To avoid false positives, we use the HSV color space, according to the color saturation, preserving image color saturation higher part, but may contain shadows, so we can be shaded shading net, followed by morphological way to repair the broken edge points to form a more complete graphics.

After the above image processing, the storage location of individual enclosed area, for individual objects and then to classify the color. The concept of pattern recognition is to strike all the pixel R, G, B three color individual means, according to the R, G, B color identification of the individual means do, Figure 6 is a color recognition value results, the recognition results described in Table 2.

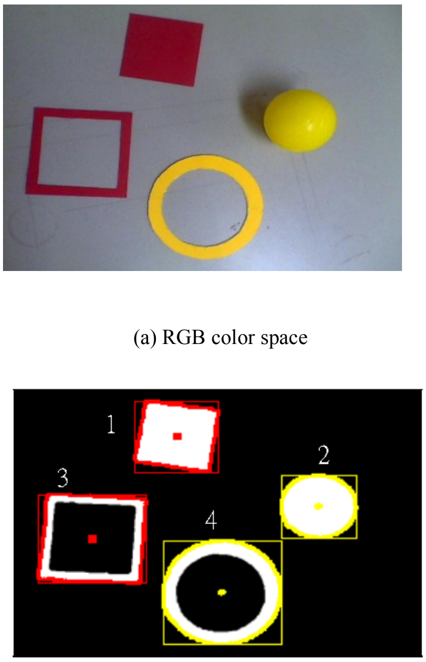

(a) RGB color space

(b) color recognition results

Figure 6. color recognition program execution results

TABLE 2 ILLUSTRATE THE RESULTS OF IMAGE RECOGNITION

	result
Graph 1	red
Graph 2	yellow
Graph 3	red
Graph 4	yellow

B. Shape Recognition

First, after pre-processing the captured image, after color space conversion, low-pass filtering, thresholding and morphological block after only black and white, how to find the target from the block and distinguish shapes. Therefore, on the identification of the area and perimeter of a graphical concept as a ratio, the calculation formula, A is the area where, P is the perimeter, the use of this measure to determine the equation square, triangular, circular and other graphics, such as table 3. Shape program execution shown in Figure 7, the results described in Table 4.

TABLE 3 GRAPHICS AREA, PERIMETER, AND MEASUREMENT VALUES

	Area(A)	Perimeter (P)	Ideal metrics (M)	Range
Circle	πr^2	$2\pi r$	1	$0.85 \leq M \leq 1$
square	r^2	$4r$	$\frac{\pi}{4} \approx 0.79$	$0.70 \leq M < 0.84$
Triangle	$\frac{\sqrt{3}}{4} r^2$	$3r$	$\frac{\sqrt{3}}{9}\pi \approx 0.6$	$0.5 \leq M \leq 0.65$

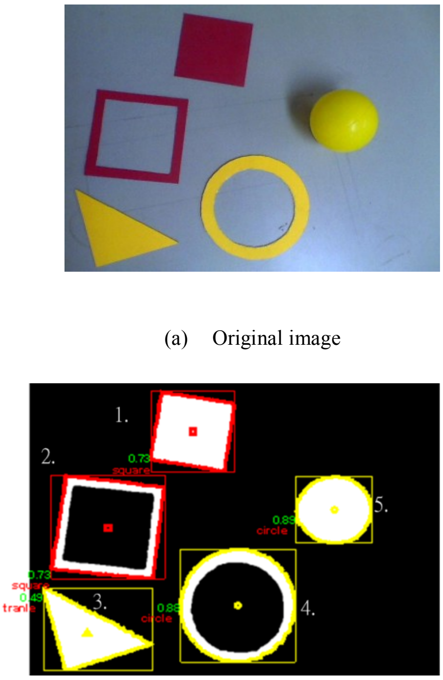

(a) Original image

(b) Recognition results

Figure 7. Shape recognition program execution results
(a) original image and (b) the recognition result

TABLE 4: RESULTS OF THE OBJECT SHAPE RECOGNITION DESCRIPTION

	metrics (M)	result
Graph 1	0.73	square
Graph 2	0.73	square
Graph 3	0.49	Triangle
Graph 4	0.88	circle
Graph 5	0.89	circle

C. Endpoint Detection

In order to be able to perform simple TicTacToe arm, it must first know the pen down the center, we must first determine the endpoints and intersections. With this camera to capture the image, through the binarization, thinning to find the image of the skeleton shown in Figure 8.

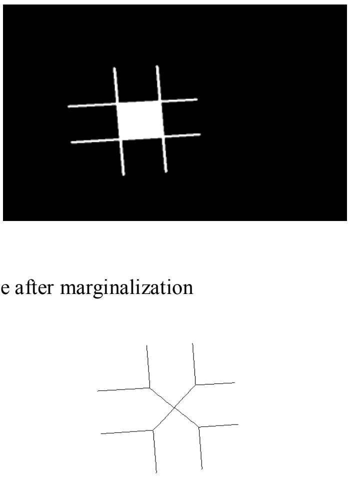

(a) fill the image after marginalization

(b) the results of thinning

Figure 8. image preprocessing execution result
(a) After the image fills marginalized (b) the results of thinning

Strike its endpoint detection method, using a 3X3 mask to scan the image, followed by a few rules to mark the endpoints and intersections, the endpoint detection program execution results shown in Figure 11, to find out the endpoint and the crossover point, you can define pen down the center, shown in Figure 12:

1) vertex, edge point: when the mask center as the black point, determine whether the neighborhood of only two black points, then this point is the vertex coordinates, as shown in Figure 9.

2) Intersection: the black mask center point, determine whether there is neighborhood four to five black spots, because there would be more black spots in the junction gathered, so long as it is established crossing point in Figure 10 shown.

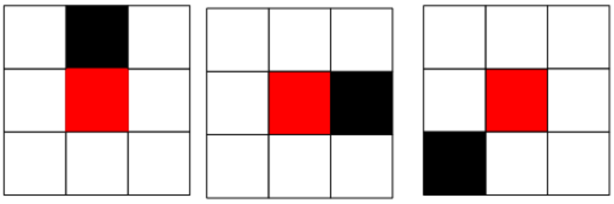

Figure 9. vertices, edges, points

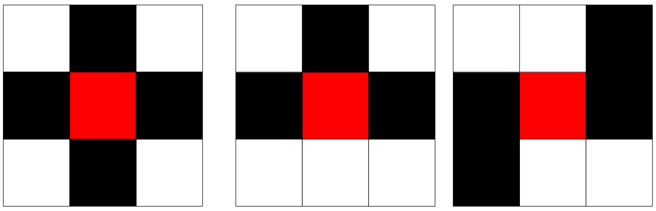

Figure 10. crosspoint

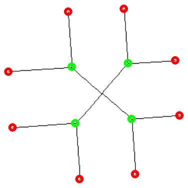

Figure 11. endpoint detection program execution results

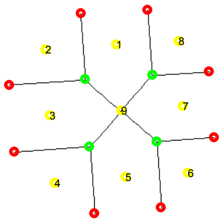

Figure 12. Tic Tac Toe pen down the center

IV. THE EXPERIMENTAL RESULTS

This article uses the robotic arm system on chip to achieve visual servo systems, including single-axis motor position control experimental transient response with S-curve trajectory planning, robot-point space motion, static target capture and placement of the robotic arm interactive Tic Tac Toe which contains the clip pen, write, put pen to control the interface shown in Figure 13.

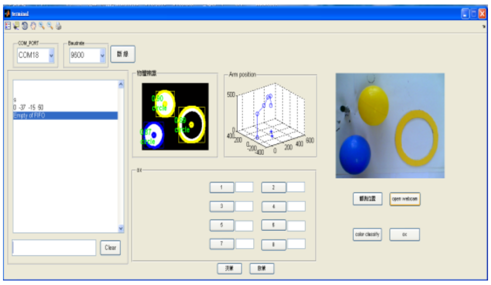

Figure 13 manipulator control interface

A. Axis motor control

As used herein, the axis of rotation of each arm DC servo motors to produce S-Curve through FPGA acceleration and deceleration curve position command pulse input command, the servo motor feedback signal configured on the optical encoder, the decoder via the FPGA decoding, and outputs the result to the PID controller, PID controller outputs the operation result to the motor driver to drive the motor, and Figure 14 is a transient response of the motor position control, Figure 15 is a S-Curve ramp position command and the motor position, exercise time 1.5 seconds.

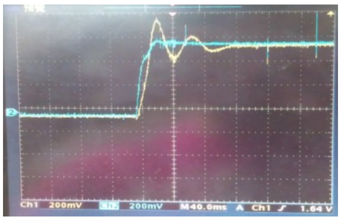

Figure 14. motor position control transient response

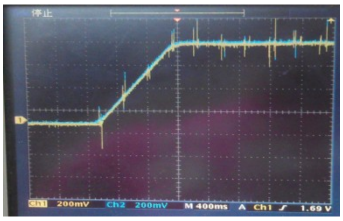

Figure 15. S-Curve acceleration and deceleration position command and the motor position, movement time is 1.5 seconds (yellow for the motor position, the blue for the command value)

B. Point space motion manipulator

In the multi-axis robot movement experiments point moving the robotic arm from the starting point (248, 0, 394) mm to the end point (320, 0, 208) mm, the angle of the axis as shown in Table 5 , the movement diagram shown in Figure 16.

TABLE 5-POINT MOVEMENT OF EXPERIMENTAL DATA

	Start point (248 ,0 ,394)mm	End point (320 ,0 ,208)mm
J1	0°	0°
J2	-35°	0°
J3	-15°	0°
J4	50°	0°

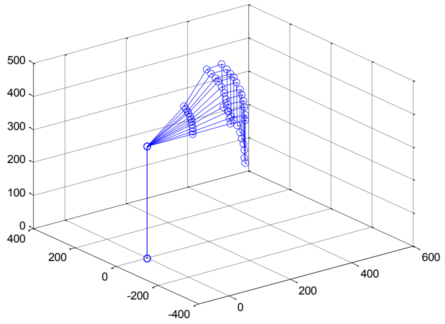

Figure 16 manipulator trajectory

C. Color of the object shape recognition

This mining monocular vision, it is in no way of knowing on the identification of the object depth, the height must be given first grab objects to correctly pick up objects, experimental procedure outlined below, desktop, yellow, blue sphere each one, place the point yellow round, first fixed arm gesture captured images will be captured image pre-processing and recognition, distinguish color and shape to classify and distinguish the placement point and the object location, identification is completed sphere coordinates and arm coordinates, Figure 17 is a manipulator object color recognition classification action.

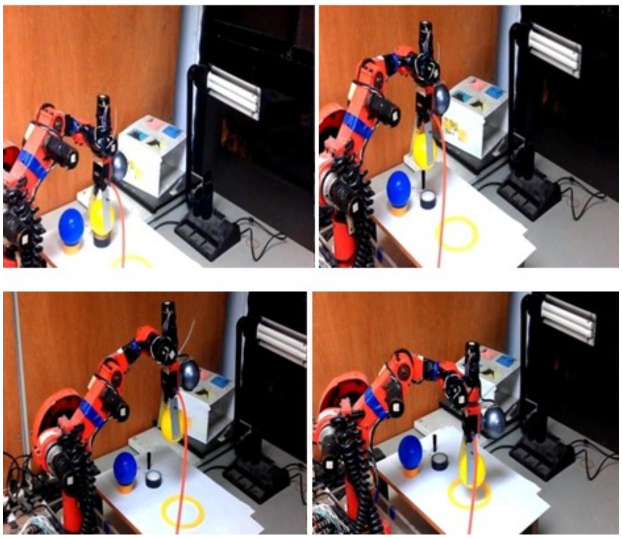

Figure 17 manipulator object color identification Categories Action

D. Arm Tic Tac Toe Game

This realization Tic Tac Toe game with image recognition, the implementation process as described below, first the fixed arm gesture captured images will be captured image pre-processing and recognition.

By endpoint and Crosspoint find pen down position, nine numbered sequentially pen down position shown in

Figure 18, the automatic brush put as a fixed position on the front panel clip pen button pressed, execute the saved locations command, Figure 19 is a clip pen movement, and can be contacted by HMI in any position to write on the sign of X o and after the completion of writing back in place after the document, complete this experiment, writing the result is shown in Figure 20.

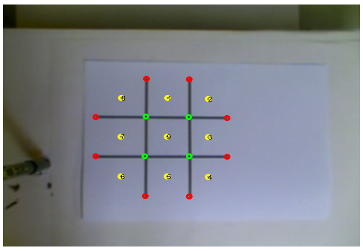

Figure 18 pound sign recognition results.

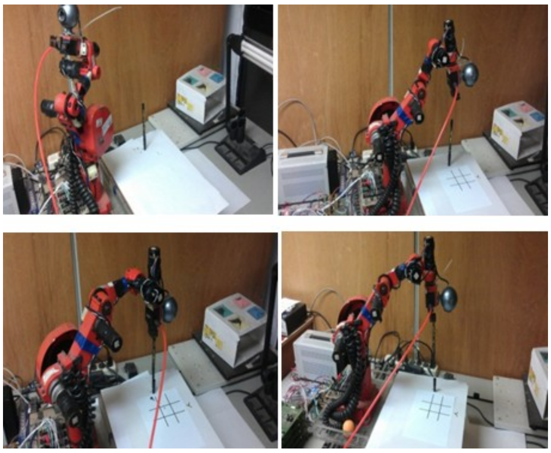

Figure 19 clip pen movements

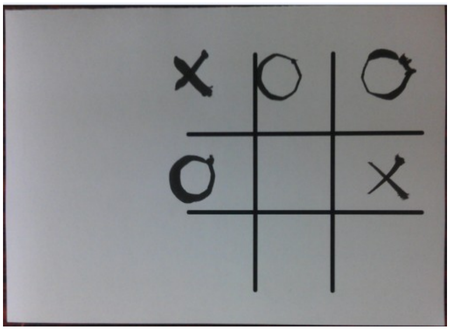

Figure 20 manipulator writing results

E. FPGA resource allocation

This paper developed using Altera's Quartus II software processing circuit synthesis, FPGA resource allocation percentage shown in Table 6. NIOS microprocessor which takes up system resources, take up more than half of the overall resource, the motor position servo control module is not related to excessive consumption of resources.

TABLE 6 FPGA RESOURCE ALLOCATION TABLE

Family	Cyclone II
Device	EP2C70F672C6
Total logic elements	7,636 / 68,416 (11 %)
Total registers	4512
Total pins	536 / 622 (86 %)
Total memory bits	257,024 / 1,152,000 (22 %)
Embedded Multiplier 9-bit elements	26 / 300 (9 %)
Total PLLs	1/4 (25%)

V. CONCLUSION

In this paper, using the system on chip as a basis for developing manipulator motion control system , this chip contains a NIOS II microprocessor and programmable logic devices . Chip design concept is simple but the speed requirements of the operational functions faster with hardware circuit , while the computational complexity and the need for flexibility to use the functions implemented by software , the two modules can be processed in parallel , so that the system has high flexibility and modification improve control performance , the completion of a robot motion control chip , this chip high portability , can be applied to different areas depending on the user , if the same controlled body and this institution , as long as the DH parameters can be modified , to complete this research project are as follows :

A. Hardware section

1) digital low -pass filter: high frequency noise suppression into the motor position control system .

2) quadruple decoding circuit: detects motor turn -degree angle .

3) PID controller: Control motor position .

4) S-curve trajectory planning: steady sending position commands.

5) pulse width modulation circuit: the control signal sent to the motor drive circuit.

B. the software part (NIOS II microprocessor)

1) Serial communication: communication with the upper user.

2) Anti- Kinematics: Using DH conversion method to calculate the movement of each axis robot arm angle, so that the terminal is moved to the target position .

3) FIFO: Enter the command will be buffered and storage .

C. image processing

1) color of the object shape recognition: according to objects by color and shape classification.

2) Tic Tac Toe: image recognition pen down the center , use the robotic arm writing o or x.

REFERENCES

[1] F. J. Lin, D. H. Wang, and P. K. Huang, “FPGA-based Fuzzy Sliding-mode Control for a Linear Induction Motor Drive,” Proceeding of the International Conference on Electrical Power Application, Vol. 152, No. 5, pp.1137-1148, September 2005.

[2] Y. S. Kung, and G. S. Shu, “Development of a FPGA-based Motion Control IC for Robot Arm,” Proceeding of the IEEE International Conference on Industrial Technology, pp.1397-1402, 2005.

[3] Monmasson E., Cirstea, M., "FPGA Design Methodology for Industrial Control Systems - A review," IEEE Trans. on Industrial Electronics, Vol. 54, No. 4, August 2007.

[4] Giuseppe Casalino, Fabio Giorgi, Alessio Turetta, and Andrea Caffaz, "Embedded FPGA-based Control of a Multifingered Robotic Hand," 2003 IEEE International Conference on Robotics & Automation, Taiwan, 2003, pp 2786-2791.

[5] X. Shao , D. Sun and J. K. Mills "A new motion control hardware Architecture with FPGA-based IC design for robotic manipulators", Proc. IEEE Int. Conf. Robot. Autom., pp.3520 -3525 2006

[6] Y. F. Chan , M. Moallem and W. Wang "Design and implementation of modular FPGA-Based PID controllers ", IEEE Trans. Ind. Electron., vol. 54, no. 4, pp.1898 -1906 2007

[7] Giuseppe Casalino, Fabio Giorgi, Alessio Turetta, and Andrea Caffaz, "Embedded FPGA-based Control of a Multifingered Robotic Hand," 2003 IEEE International Conference on Robotics & Automation, Taiwan, 2003, pp 2786-2791.

[8] G. N. Desouza and A. C. Kak, “Vision for mobile robot navigation: a Survey,” IEEE Transactions on Pattern Analysis and Machine Intelligence, Vol. 24, pp. 237-267, Feb. 2002.

[9] J. H. Jean, T. P. Wu, J. H. Lai, and Y. C. Huang, “A visual servo system for object tracking applications of mobile robots based on shape features,” Proceedings of 2005 CACS Automatic Control Conference Tainan, Taiwan, Nov 18-19, 2005.

[10] ALTERA, “Nios II Software Developer’s Handbook,” ALTERA Corporation

[11] NIOS Embedded Peripherals IP User Guide, ALTERA Corporation, 2003.

[12] DE2 Development and Education Board User Manual, ALTERA Corporation, 2003.